INFLUENCE OF IONIZING RADIATION ON THE STOCHASTICITY OF OVERVOLTAGE PROTECTION AT LOW, MEDIUM, AND HIGH VOLTAGE LEVELS IN GAS SURGE ARRESTERS

by

Alija R. JUSIĆ [1*]***, Djordje R. LAZAREVIĆ*** [2]***, and Irfan M. TURKOVIĆ*** [3]

[1] Power Electric Utility of Bosnia and Herzegovina, Sarajevo, Bosnia and Herzegovina
[2] Electrical Engineering Institute Nikola Tesla, University of Belgrade, Belgrade, Serbia
[3] Faculty of Electrical Engineering, University of Sarajevo, Sarajevo, Bosnia and Herzegovina

Scientific paper
https://doi.org/10.2298/NTRP2301018J

The paper considers the possibility of improving the technical characteristics of gas surge arresters for the co-ordination of insulation at low voltage, medium voltage and high voltage levels. The idea for improving the characteristics of a gas surge arrester is based on the application of the radioactive source ^{241}Am in the area of the surge arrester cathode. Intensive ionization with alpha particles significantly increases the number of free electrons in the space between electrodes, which shortens the time of their transition to initial electrons. This changes the Paschen curve of the gas surge arrester, narrows and flattens its impulse characteristic and reduces the stochasticity of the response of the gas surge arrester. All this results in a significant improvement in the characteristics of the gas surge arrester at all voltage levels. This improvement is particularly noticeable in the case of low voltage surge arresters. The paper is basically theoretical-experimental research. The experiments were performed under well-controlled laboratory conditions. The combined measurement uncertainty of all measurements was acceptable.

Key words: gas surge arrester, insulation coordination, low, medium, and high voltage levels, response improvement

INTRODUCTION

The principle of overvoltage protection is to connect the components, which are protected, in parallel with the overvoltage protection. The surge protection should meet the requirements: has an infinite resistance for voltages lower than the nominal voltage of the component being protected, it has a low resistance for voltages higher than the nominal voltage of the component being protected, and the capacitance is significantly lower than the capacitance of the components being protected.

The principles of overvoltage protection are the same, regardless of the voltage level at which protection is performed. For this reason, the components for overvoltage protection are the same, or rather very similar [1-3]. The most important parameters of the quality of protective components are: speed of response, tolerable current, and reversibility of characteristics after operation [4, 5].

Overvoltage protection components are: diodes, varistors, and gas surge arresters. Diodes are the fastest surge arresters. Their disadvantage is the relatively low value of the current they can conduct (low power). Likewise, a disadvantage is the relatively frequent possibility of destruction, with the loss of the ability to perform the protection function. Varistors have a slower response than diodes. They can conduct a significantly higher current without irreversible changes in characteristics. However, if the current that the varistor conducts is much higher than the minimum value, irreversible changes can occur in its characteristics and possibly destruction (with the loss of the protection function). The slowest of all surge protection components are gas surge arresters. However, gas surge arresters have an unlimited ability to conduct a current with small irreversible changes (while retaining the protective function). As a disadvantage of gas surge arresters, it is often stated that the value of the nominal breakdown voltage is a stochastic quantity. It shows that the stochasticity of the value of the nominal breakdown voltage depends on the shape of the overvoltage pulse [6]. In addition to surge protection components, hybrid circuits containing different types of filters (together with surge protection components) are often used [7, 8]. The aim of this paper is to examine the possibility of improving the characteristics of gas surge arresters by applying ionizing radiation.

* Corresponding authors, e-mail: al.jusic@epbih.ba

GAS SURGE ARRESTERS

Gas surge arresters work on the principle of electrical breakdown of gases. The manner of functioning, advantages and disadvantages of gas surge arresters do not depend on the voltage level for which they are designed. However, the methods that could influence the characteristics of gas surge arresters differ due to the different breakdown mechanism between gas surge arresters for the low voltage level, gas surge arresters for the medium voltage level and high voltage level. Namely, gas surge arresters that are used for co-ordination of insulation at the low voltage level work in the area of the combined breakdown mechanism where the gas breakdown takes place by the anomalous Paschen effect, the Townsend mechanism and the streamer mechanism. Gas surge arresters used for insulation co-ordination at the medium and high voltage level work in the area of the streamer breakdown mechanism [9, 10]. The anomalous Paschen gas breakdown mechanism occurs in the border regions between the vacuum breakdown mechanism and gas breakdown mechanism. In that area, the breakdown takes place by a mechanism that is essentially close to the Townsend mechanism. That is, for the self-maintenance of the avalanche mechanism of electric discharge in the case of the Paschen mechanism, secondary processes active on the electrodes (ion discharge, photoemission, discharge with metal ions) are necessary. The primary processes in the case of the anomalous Paschen breakthrough mechanism are processes active in the gas (ionization by positive ions, photoionization, ionization by metastable atoms or ions). The only difference between the anomalous Paschen mechanism and the Townsend mechanism is that the breakdown in the case of the anomalous Paschen minimum does not take place along the shortest electric field line (*i. e*., the line of maximum electric field) but along some longer field line that provides minimum energy consumption. The anomalous Paschen breakdown mechanism occurs at points to the left of the Paschen minimum and leads to flattening of the Paschen curve, *i. e*., to a constant value of the breakdown voltage. Such a phenomenon is a consequence of the fact that Paschen's curve is the dependence of the value of the breakdown voltage on the product of pressure and interelectrode distance (*i. e*., pressure and the length of the trajectory of the spark that makes the breakdown), [11, 12]. The Townsend breakdown mechanism is characteristic for points to the right of the Paschen minimum in the regions of the product of pressure and interelectrode distance close to the minimum. This means that the Townsend breakdown mechanism occurs at the rising points of the Paschen curve. The primary processes of electrical breakdown by the Townsend mechanism are active in the gas, and the secondary processes are active at the electrodes. In this way, the breakdown mechanism does not differ from the breakdown mechanism by the anomalous Paschen mechanism. Breakdown by the anomalous Paschen mechanism and breakdown by the Townsend mechanism occur at underpressure of the order of 10^{-4}-10^{-10} Pa and small values of the interelectrode distance (0.1-1 mm).

Electric breakdown by the streamer mechanism occurs when the density of electrons created by the primary processes of electric discharge in gases equals the electron density of the primary avalanche. This effect occurs when the amount of charge in the primary avalanche reaches a sufficient value to significantly increase the field in the direction of the electrodes, which leads to the ionization phenomenon in the gases. These ionization phenomena thus generate the free electrons needed to maintain the avalanche breakdown. The streamer breakdown is characterized by a large number of partially ionized channels (streamers) that arise in the interelectrode space. When one streamer bridges the interelectrode space, a current flows through it. This current, by the Joule effect, heats the streamer and leads to thermoionization of the gas in it. The appearance of the thermoionization of the channel bridging the interelectrode space creates the conditions for a breakthrough by the streamer mechanism [13]. The streamer mechanism is active in all areas where the Townsend mechanism does not occur. From the aspect of gas surge arresters, it is important to note that the mechanism of the gas breakthrough in low voltage arresters is of the Townsend type, and in the case of medium voltage and high voltage arresters of the streamer type. Considering the mechanisms of gas breakdown, it was assumed that there is an electric field in the interelectrode space that allows the electron on the mean free path length to gain energy to ionize the atoms of the insulating gas molecule. Such a field value is called critical. This kind of breakdown can be realized with all types of voltage. Especially important are DC and impulse voltage types. The DC breakdown occurs when the rate of change of the electric field is much higher than the rate of elementary electrical discharge processes in gases. Impulse breakdown occurs when the rate of change of the electric field is of the same order of magnitude as the rate of elementary electrical discharge processes in gases. The DC breakdown voltage is a deterministic quantity, *i. e*., type A measurement uncertainty for its experimental determination is zero. The impulse breakdown voltage is a stochastic quantity, *i. e*., type A measurement uncertainty for its experimental determination is greater than zero [14, 15].

Since overvoltage phenomena in networks at all voltage levels occur in pulse form (standard impulse voltage 1.2/50 μs for lightning impulse overvoltage and 250/2500 μs for switching overvoltage, approximately) special attention should be paid to impulse breakdown. Figure 1 shows the impulse wave shape of the gas breakdown.

In fig. 1, t_p is the statistical time. The statistical time is the time that elapses from exceeding the value of the DC breakdown voltage U_B to the appearance of

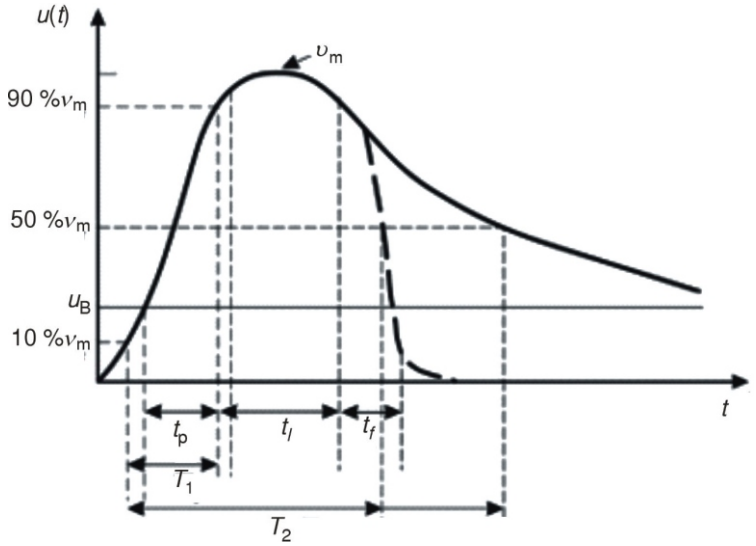

Figure 1. Characteristic wave shape of impulse voltage with which the breakdown was achieved

the initial electron. The t_l is the time of avalanche formation, *i. e*., time from the appearance of the first avalanche to the formation of the main discharge. In the same figure, t_f is the so-called formative time required for the formation of the thermal channel of the spark [16].

Unlike the value of the DC breakdown voltage, which can be determined numerically, the impulse breakdown voltage is characterized by so-called impulse characteristics. The impulse characteristic represents a smooth curve in the voltage-time plane where the impulse breakdown voltage value of a certain probability quantile is expected to be. In order to experimentally determine the impulse characteristic, a very large number of measurements (theoretically an infinite number of measurements) of the impulse breakdown voltage would be required. Since this is practically impossible, the law of surfaces is used in practice [17, 18].

DETERMINATION OF IMPULSE CHARACTERISTICS USING THE LAW OF SURFACES

The stochasticity of the random value of the impulse breakdown voltage results from stochasticity of statistical time, fig. 1. Namely, in the interelectrode space there are always free electrons that are created by collision processes [19]. However, these free electrons are not necessarily initial electrons.

Namely, in order for a free electron to become the initial electron, it needs to be in a place in the electric field where it can, on one length of the free path, take over from the field enough energy to start the avalanche process. Since this process takes place in time, a time-dependent impulse characteristic is obtained.

Experimental determination of impulse characteristics is very difficult. It is impossible because for small probability quantiles it is associated with an extremely large number of measurements with different wave shapes of impulse voltages. For this reason, a semi-empirical method based on the law of surfaces is used to determine the impulse characteristics. The same law can be applied to the determination of the minimum withstand voltage of arbitrary gas insulation [20, 21].

The law of surfaces is derived based on the proven fact that the plasma velocity in the interelectrode space is proportional to the value of the electric field

$$v(x,t) \quad k[E(x,t) \quad E_{\mathrm{B}}] \tag{1}$$

where x is the spatial co-ordinate, t – the time, k – the constant of proportionality, and E_{B} – the electric field that corresponds to the DC break down voltage U_{B}.

The electric field can be represented as a product of two functions

$$E(x,t) \quad u(t)g(x) \tag{2}$$

where $g(x)$ is a function determined by the electrode configuration.

After distributing the variables x and t, the integration can be performed

$$\frac{1}{k}\int_{t_1}^{t_1+t_2}\frac{\mathrm{d}x}{g(x)} \quad \int_{t_1}^{t_1+t_2}[u(t) \quad U_{\mathrm{B}}]\,\mathrm{d}t \tag{3}$$

where t_1 is the moment in time when the impulse voltage becomes equal to the value of the DC breakdown voltage U_{B}, and $t_1 + t_2$ – the total time of the impulse breakdown.

Based on eq. (3), it can be concluded that there is a constant surface between impulse voltage $u(t)$ and voltage U_{B}, during breakdown t, fig. 2.

This conclusion makes it possible to determine, on the basis of a representative statistical sample obtained by one form of impulse voltage, the impulse characteristics of an arbitrary quantile of probability for these forms of impulse voltage. The procedure for determining the impulse characteristics based on the law of surfaces is to fit the random variable value of the impulse breakdown voltage with the best theoreti-

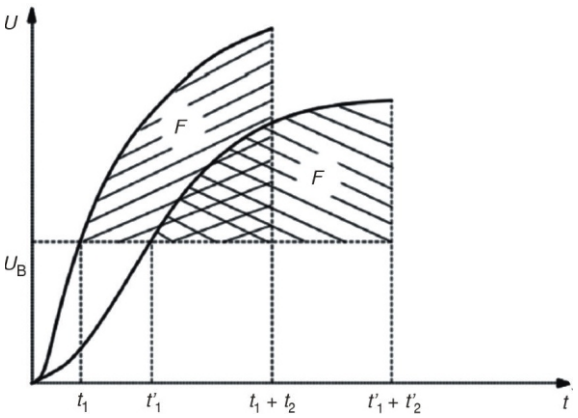

Figure 2. Graphic interpretation of the voltage-time plane where the law of surfaces applies (where *F* is a constant area in the voltage-time plane)

cal statistical distribution: the value of the impulse breakdown voltage for the desired probability quantile is taken from the obtained distribution, calculation of times t_1 and $t_1 + t_2$ based on the known wave shape of the impulse voltage and the value of the DC breakdown voltage U_B, calculation of the area between the impulse voltage and the DC breakdown voltage value for the desired probability quantile based on eq. (3), and calculation of the impulse characteristic for the desired probability quantile. The described procedure for calculating the impulse characteristics is very important in the case of small probability quantiles, since the corresponding values are difficult to determine experimentally [22]. In engineering practice, two impulse characteristics are usually determined by the 0.1 % and 99.9 % quantile probability. In this way, an area is obtained in the voltage-time plane where almost all values of the impulse breakdown voltage are located (regardless of the form of the impulse voltage).

EXPERIMENT

Since the impact of ionizing radiation on the response of gas surge arresters at low voltage, medium voltage and high voltage levels is considered in the paper, three models of gas surge arresters were used for the range of product values *pd* (pressure *x* interelectrode distance) and for three voltage levels. The gas surge arrester model for the low voltage level is designed for the pd value from 10^{-4} bar mm to 1 bar mm (1 bar = 100 kPa). Variable pressures ranged from 1 mbar to 1000 mbar, and the interelectrode distance from 0.1 mm to 1 mm. The zero distance between electrodes was determined by measuring the ohmic resistance. The interelectrode distance was adjusted with a high-precision (electronic) micrometer system. The measurement uncertainty of setting the working *pd* point of such procedure type B was 0.3 % [23, 24]. Figure 3(a) shows a schematic diagram of

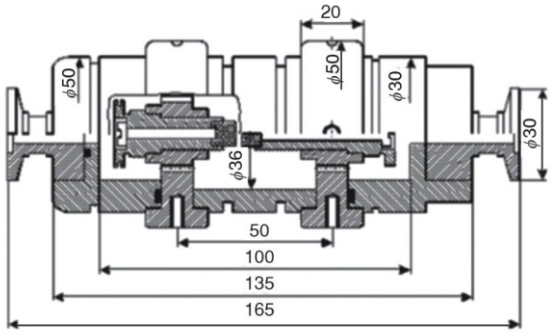

Figure 3(a). Cross-section of a gas surge arrester model for low voltage insulation co-ordination

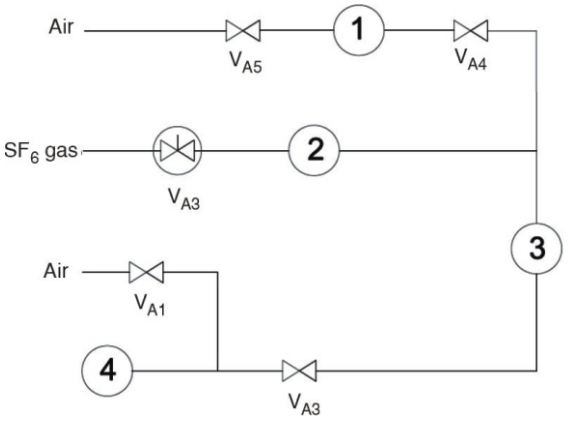

Figure 3(b). Diagram of the gas circuit for adjusting the pressure of the SF6 gas in the gas arrester model for the coordination of the insulation at the low voltage level; 1 – gas surge arrester model, 2 – mechanic vacuum pump, 3 – diffusion vacuum pump, and 4 – molecule vacuum pump, are two-position valves, is a dosing valve (needle valve)

the chamber-model of a low voltage gas surge arrester. The chamber-model from fig. 3(a) is designed for negative pressure. The overpressure in the chamber is set to a value corresponding to the temperature of 0 °C. The purity of gas in the chamber was extremely high. Namely, the chamber was repeatedly vacuumed and flushed with working gas before filling with working gas to the set pressure (which was reduced to the appropriate value at 0 °C). Figure 3(b) shows the gas circuit for filling the chamber. The interelectrode distance was variable. For each distance, other pairs of Rogowski electrodes were made in accordance with the laws of similarity for gas discharge [25, 26].

Rogowski type electrodes provided a pseudo-homogeneous electric field, but without the undesirable edge effects. Chamber sealing was extremely reliable. This was achieved by applying adequate procedures and it worked despite the extremely small atom of He gas with which the chamber was filled. A hole was made at the cathode of the chamber with a width larger than the mean free path length of electrons in the gas at the working pressure (this was done to take advantage of the hol-

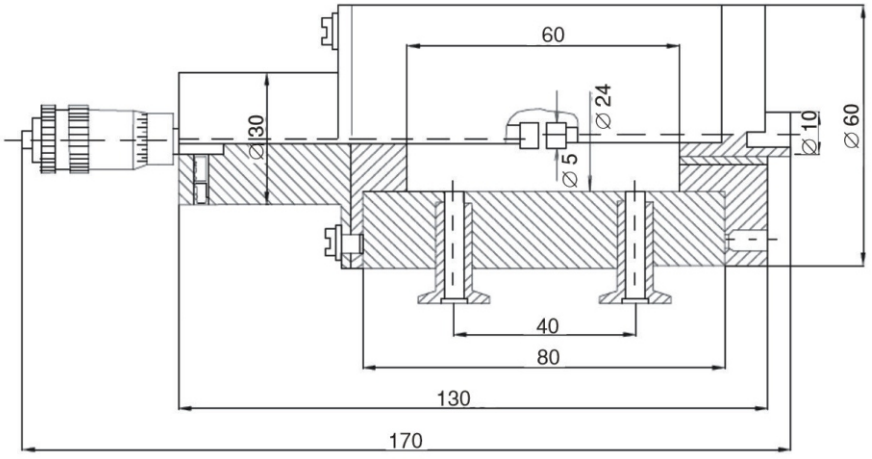

Figure 4(a). Cross-section of a gas surge arrester model for medium voltage insulation coordination

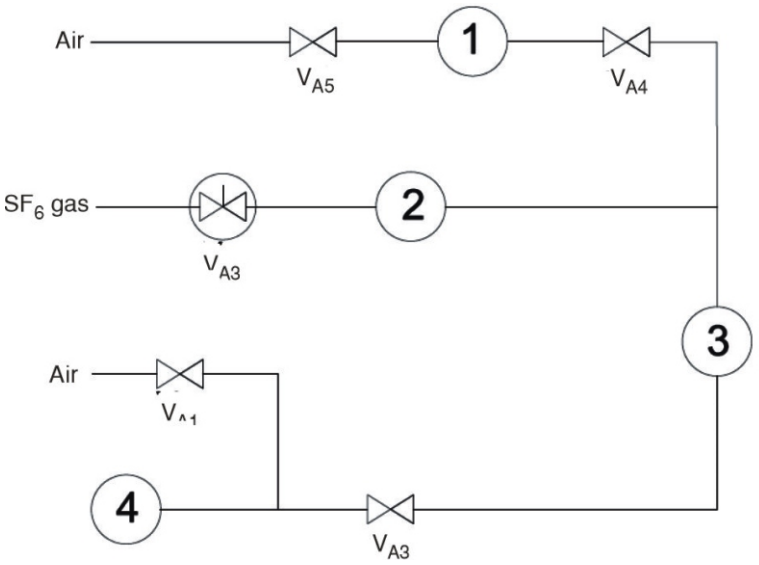

Figure 4(b). Diagram of the gas circuit for adjusting the pressure of the SF6 gas in the gas arrester model for the coordination of the insulation at the medium voltage level; 1 – gas surge arrester model, 2 – mechanic vacuum pump, 3 – diffusion vacuum pump, and 4 – molecule vacuum pump, are two-position valves, is a dosing valve (needle valve)

low cathode effect [27]). A radioactive source of ^{241}Am was placed in that hole, emitting a-particles. The ^{241}Am source was screened at the electrode potential to be protected against spark shock during breakdown. The gas surge arrester model for the medium voltage level is designed for a product value pd from 1 bar mm to 20 bar mm. The applicable pressures ranged from 1 bar to 4 bar, and the interelectrode distance from 1 mm to 10 mm. The cathode was mounted on an external micrometer screw and then fixed. The zero interelectrode distance was determined by measuring the ohmic resistance. The interelectrode distance was determined by a micrometer screw to which a variable cathode was attached. Type B measurement uncertainty was observed at 0.4 % [28]. Figure 4(a) shows a model of the medium voltage gas surge arrester chamber. Figure 4(b) shows the gas circuit for filling the model chamber.

The chamber-model of the gas surge arrester was designed for overpressures (when designing for overpressures and underpressures, it is important to properly profile the O-rings). The pressure in the chamber was adjusted to 0 °C the purity of the gas in the chamber was extremely high. Namely, the chamber was repeatedly vacuumed and flushed with a working gas before filling with a working gas for the set pressure to the appropriate value reduced to 0 °C. The interelectrode distance was variable.

Rogowski electrodes were used. As in the case of the chamber-model, for each interelectrode distance, another pair of electrodes was used in accordance with the law of similarity for gas discharges. The chamber-model of medium voltage surge arresters did extremely well. The fact that the working gas was SF6 also contributed to this.

The chamber-model gas surge arrester for high voltage level is designed for product value *pd* from 10 bar mm to 300 bar mm. Applied pressures ranged from 1 bar to 6 bar, and the interelectrode distance from 10 mm to 30 mm. Zero distance between the electrodes was determined by measuring the ohmic resistance. Interelectrode distance was determined by precise threading of the cathode support. Type B measurement uncertainty of the operating point adjustment was 0.5 %. Figure 5(a) shows the diagram of the chamber-model of the high-voltage gas surge arrester. The chamber-model from fig. 5(a) is designed for overpressures. The pressure in the chamber is set to overpressure as in the case of the chamber-model of the low-voltage arrester. Figure 5(b) shows dia-

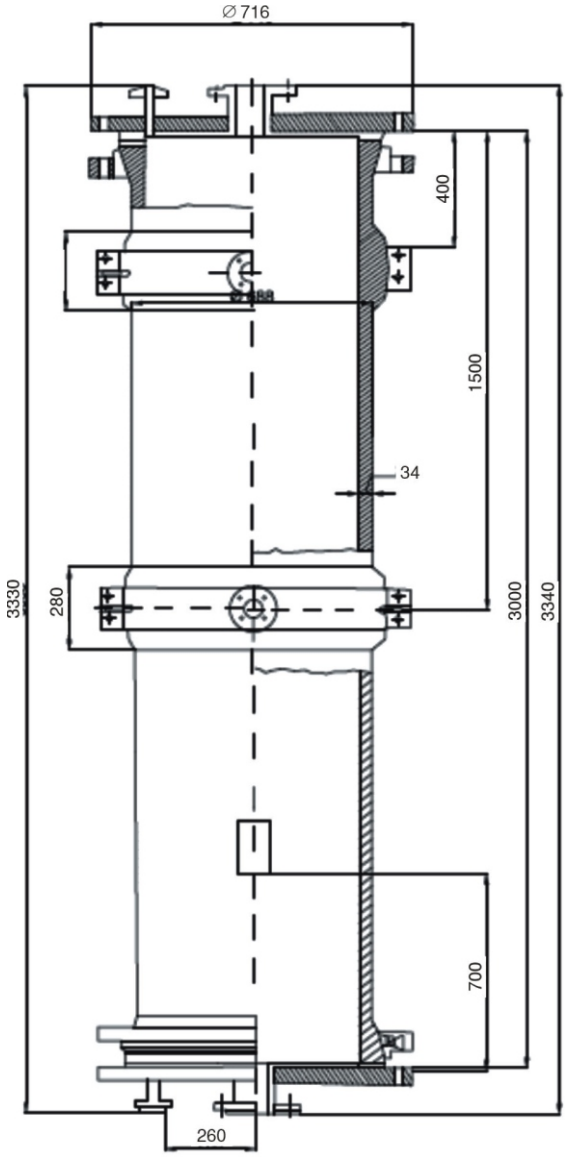

Figure 5(a). Cross-section of a gas surge arrester model for high voltage insulation coordination

gram of the gas circuit for adjusting the pressure of the SF6 gas in the gas arrester model for the co-ordination of the insulation at the high voltage level.

In all chambers the described electrodes of the Rogowski type were used. The Rogovski-type electrodes used in all chambers satisfied the law of similarity for electrical discharges in gases. The electrodes were always made of tungsten. Tungsten as a material provided optimal synergy between the melting point and thermal conductivity which minimized the change of topography of electrode surfaces during multiple breakdowns. In this way the irreversibility of characteristics of the isolation system that was experimented with was achieved. In order for this effect to be even less noticeable, the chamber-model was grounded through a resistance of 100 M , which significantly reduced the spark current.

In the case of the chamber-model for low voltage level a scheme of the pulse generator given in fig. 6 was used. The generator was adjusted so that it could give pulses of approximately 1 kV (s)$^{-1}$, 2 kV (s)$^{-1}$, 3 kV (s)$^{-1}$, 5 kV (s)$^{-1}$, 10 kV (s)$^{-1}$, 20 kV (s)$^{-1}$, 30 kV (s)$^{-1}$, 50 kV (s)$^{-1}$, 100 kV (s)$^{-1}$ and 200 kV (s)$^{-1}$.

The value of the DC breakdown voltage required to determine the impulse characteristics was determined mathematically using the conditions for the Townsend breakdown mechanism and the streamer breakdown voltage with the help of known values of Townsend coefficients [29, 30].

For that procedure, the required value of the field in the interelectrode space was determined by the charge simulation method [31].

For the chamber-model of the high-voltage surge arrester a multi-stage Max generator, fig. 7, was used and on the Max generator it was possible to obtain voltages of 100 kV (s)$^{-1}$, 200 kV (s)$^{-1}$, 435 kV (s)$^{-1}$ and 640 kV (s)$^{-1}$ by combining resistance values.

The generator and associated resistors were of the commercial type from Hetely. The value of the DC

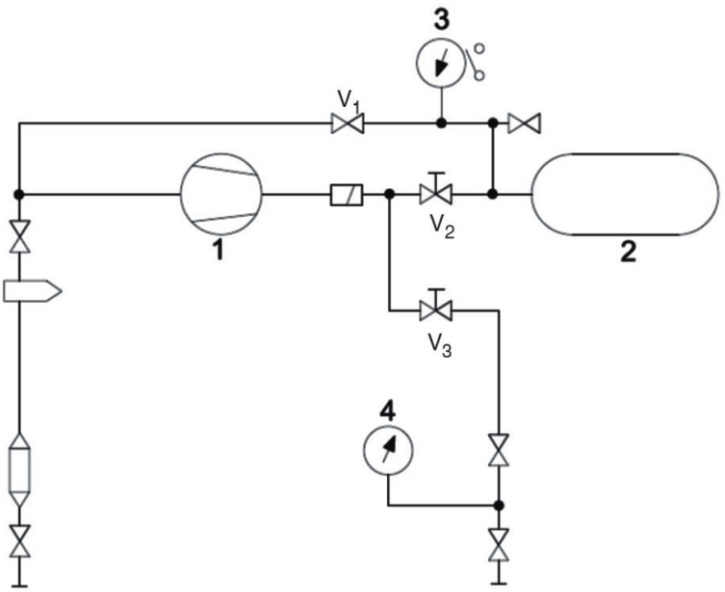

Figure 5(b). Diagram of the gas circuit for adjusting the pressure of the SF6 gas in the gas arrester model for the coordination of the insulation at the high voltage level; 1 – gas surge arrester model, 2 – mechanic vacuum pump, 3 – diffusion vacuum pump, and 4 – molecule vacuum pump, are two-position valves, is a dosing valve (needle valve)

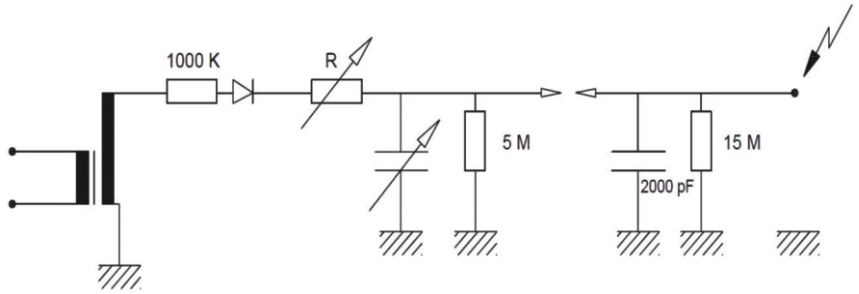

Figure 6. Diagram of the pulse generator used for low-voltage testing

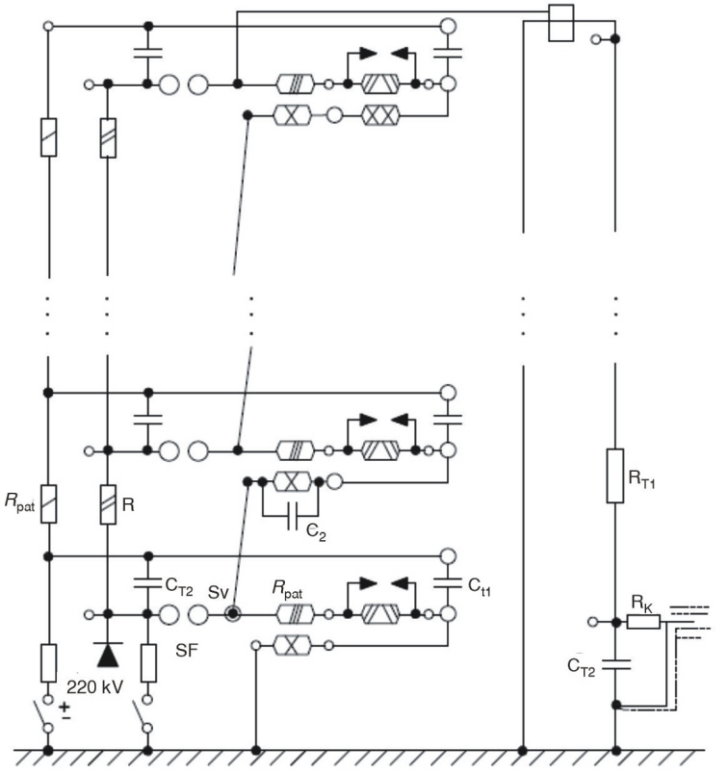

Figure 7. Scheme of the standard Max generator

breakdown voltage was determined numerically by a mathematical procedure for the needs of the impulse characteristics of the chamber-model of the low voltage surge arrester. The measurement procedure itself for all chamber-models consisted of measuring 100 impulse breakdown voltage values with breaks between two consecutive 1 minute breakdowns. With each form of impulse voltage 100 measurements were made.

The statistical processing of the experimental results within one statistical sample of the random variable impulse breakdown voltage is performed as follows: by applying the Chauvin criterion of rejecting suspicious measurement results.

By applying the *U*-test to subsamples of 10 chronological samples each, the affiliation of these random variables with a simple statistical sample was checked; determination of the first, second and third central moment of the statistical sample; the statistical distribution of random variables was determined on the basis of maximum statistical reliability, and application of the χ^2-test and the Kolmogorov test for checking the belongingness/affinity? of the random variable impulse breakdown voltage to the obtained statistical distribution. All experimental procedures were performed under well-controlled laboratory conditions. For all experimental procedures, the combined measurement uncertainty was less than 8 %.

CALCULATION OF THE ELECTRIC FIELD IN THE INTERELECTRODE SPACE AND CALCULATION OF THE DC VOLTAGE VALUE

Knowing the electric field in the interelectrode space is important for any quantitative analysis of the electric discharge process in the interelectrode space. It should be borne in mind that the initial distribution of the field will be significantly changed by the spatial

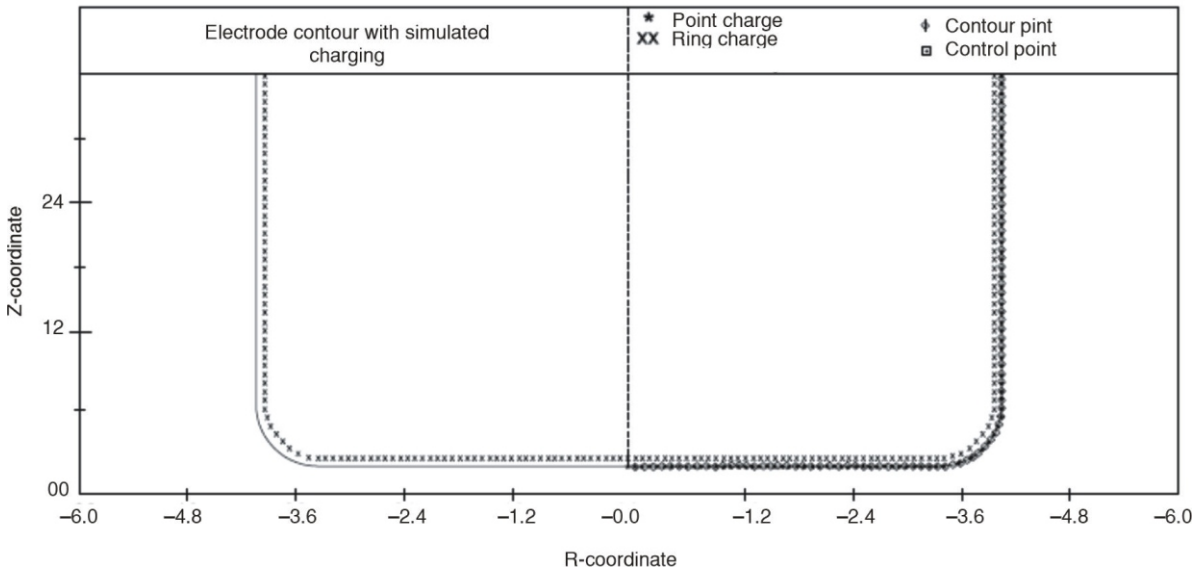

Figure 8. Cylindrical electrodes with fictitious charges contour and control points

electrification created during development of the breakdown [32].

The evaluation of non-analytical spatial distribution of the field in the interelectrode space, by the analytical sample method, using analogue analytical networks and the use of probes [33] is replaced by more adaptable and accurate numerical methods of the Laplace equation with the use of digital computers. In that case, with the exception of the geometry of flat, cylindrical and spherical coordinates, when comfort mapping also gives satisfactory results, either the finite difference method or MK or the electrification simulation method is used [34].

The finite difference method is based on an iterative procedure in which the interelectrode space is divided into a grid of variable pitch. The potential of each step is determined by successive approximations whose convergence can be improved by applying over-relaxation or accelerated finite difference formulas.

This method is effective in calculation of axisymmetric 3-D systems, but in asymmetric systems the field becomes too complex.

The program for calculation of electric fields consists of inserting a number of fictitious (simulated) charges and the same number of control points based on analytical, geometrically defined, arc, long, spiral, parabolic and hyperbolic elements of the electrode contours, fig. 8.

Determining the course of the field lines is accomplished by connecting points known to lie on it with straight lines, fig. 8. Control points allow field lines to be checked with predetermined accuracy. Once the field lines in the interelectrode space are determined, then, based on the expected breakdown mechanism, minimum voltage value, DC voltage value, that lead to breakdown is calculated. This process is done in an iterative procedure. Figure 9 shows a block diagram of the DC breakdown voltage calculation using the mentioned procedure.

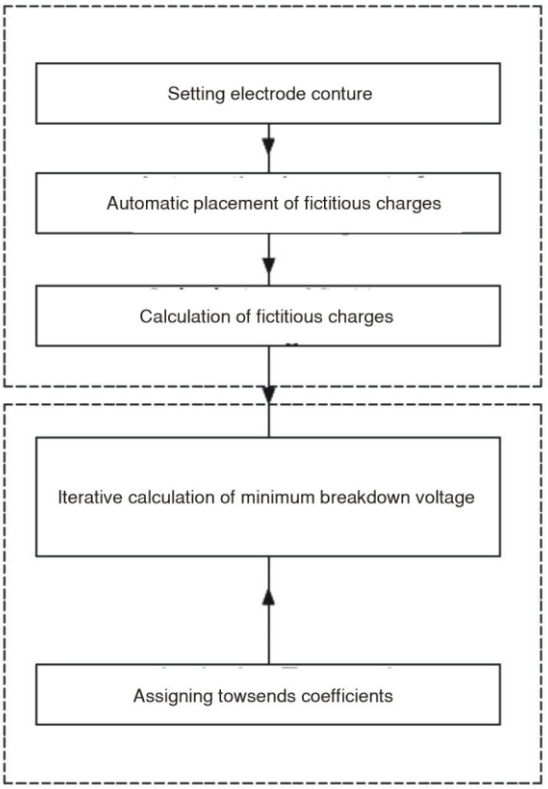

Figure 9. Diagram of the DC breakdown voltage calculation using the mentioned procedure

As for checking the correctness of fulfillment of breakdown conditions, it takes place in the following steps:

– Selecting the starting point of the field line along which the fulfillment of the breakdown conditions will be checked (it is done in such a way that for breakdowns to the right of the *P* minimum, the maximum field point is automatically adopted, and for breakdowns to the left of the *P* minimum it is set separately).

– Calculation of the field line corresponding to the starting point.
– Calculation of integral $\int_0^d \alpha(x_i)\mathrm{d}x_i$, where d is the interelectrode distance and $\alpha(x_i)$ the first Townsend coefficient, along the isolated field line. This integration after replacing the integral with the sum $\sum_{i\ 1}^{u} \alpha(x_i)\ x_i$ where u is the number of points of the observed line of the field, and x_i is their distance. The value of $\alpha(x_i)$ would be obtained based on the Townsend mechanism.
– Verification of fulfillment of breakdown conditions based on the expected breakdown mechanism.

RESULTS AND DISCUSSION

Figure 10 shows the characteristics obtained by the chamber-model gas surge arrester for the low-voltage level (for the co-ordination of insulation at the low-voltage level). The picture clearly shows that the 0.1 % and 99.9 % pulse characteristics obtained for the same conditions are wider than the corresponding pulse characteristics in which the cathode contained a source of radioactive radiation. This effect is important for engineering practice as it provides a determined operating voltage. Such a result corresponds well with the results shown by the Paschen curves.

Figure 11 shows the impulse characteristics obtained by the chamber-model gas surge arrester at the medium voltage level (co-ordination of insulation at the medium voltage level). The effect of ionizing radiation is much more visible in the picture. It can be concluded, from fig. 9, that the effect of ionizing radiation in the gas surge arrester model largely excludes the possibility that the surge passes the protection and penetrates, with destruction, to the protected element.

Figure 12 shows the impulse characteristics obtained by the chamber-model of the gas surge arrester for the high-voltage level (for the co-ordination of insulation at the high-voltage level). In fig. 12, the effect of ionizing radiation is so noticeable that it almost completely provides protection to the protected element, *i. e.*, a high-voltage gas arrester with a radioactive source provides almost complete protection for the protected element (except for some very fast overvoltages that occur during nuclear explosions in the atmosphere).

The main purpose of the surge arrester to co-ordinate all voltage levels must be reliability and must not allow the surge to pass to the protected element. However, since the voltage response of a gas surge arrester is a stochastic quantity, the problem of protection with it is the occurrence of stochastic peaks. For this reason, the question of whether ionizing radiation affects the reduction of stochastic peaks of the gas arrester and thereby increases its reliability is of interest.

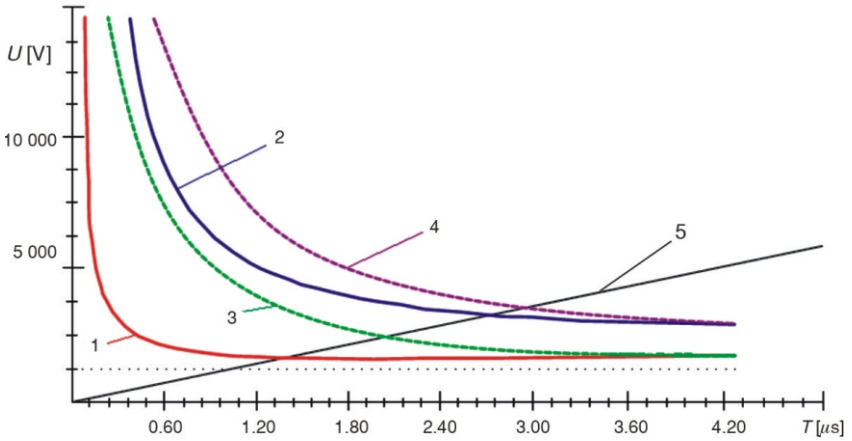

Figure 10. Impulse characteristics of 0.1 % and 99 % quantiles obtained by the method of surface constancy for gas surge arrester models on a low-voltage level: without the application of the ionizing radiation source (lines 1 and 2, respectively), with the application of the ionizing radiation source (3 and 4, respectively), and impulse voltage (5)

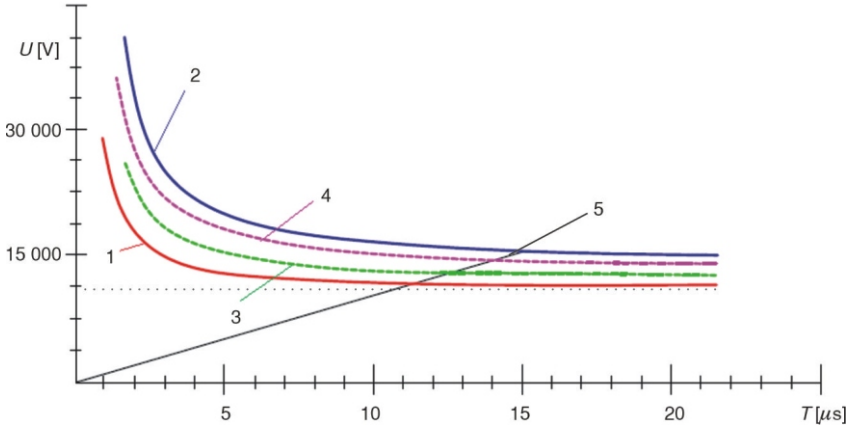

Figure 11. Impulse characteristics of 0.1 % and 99 % quantiles obtained by the method of surface constancy for gas surge arrester models on the medium-voltage level: without the application of the ionizing radiation source (1 and 2, respectively), with the application of the ionizing radiation source (3 and 4, respectively), and impulse voltage (5)

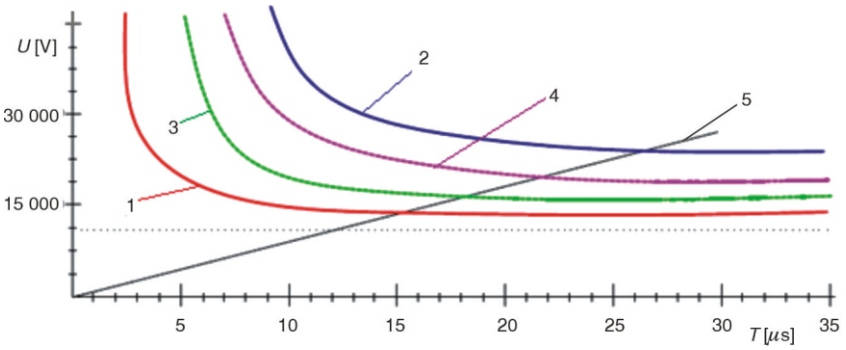

Figure 12. Impulse characteristics of 0.1 % and 99 % quantiles obtained by the method of surface constancy for gas surge arrester models on the high-voltage level: without the application of the ionizing radiation source (1 and 2, respectively), with the application of the ionizing radiation source (3 and 4, respectively), and impulse voltage (5)

Figure 13 shows the stochasticity of the response of the gas surge arrester without the application of the ionizing radiation source and with the application of ionizing radiation. From fig. 13 it is obvious that the effect of ionizing radiation significantly reduces the occurrence of stochasticity in the response of the gas surge arrester and thus significantly increases its efficiency in protection against overvoltages at the low voltage level.

Figure 14 shows the stochasticity of the response of the gas surge arrester for the medium voltage level without the application of the ionizing radiation source and with the application of ionizing radiation. In the case of a gas surge arrester, the effect of ionizing radiation on the stochastic response of the gas surge arrester for insulation co-ordination decreases significantly. It is, in relative terms, much smaller than the repetitive stochasticity that occurs in a low-voltage surge arrester.

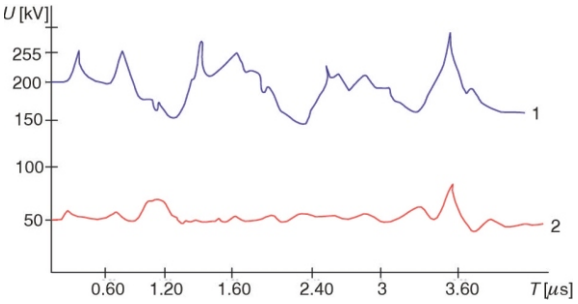

Figure 13. Stochasticity of the response of the gas surge arrester for the low-voltage level; 1 – without the application of the ionizing radiation source and 2 – with the application of ionizing radiation

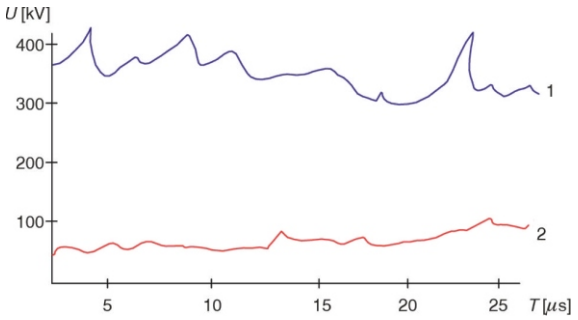

Figure 14. Stochasticity of the response of the gas surge arrester for medium-voltage level; 1 – without the application of ionizing radiation source and 2 – with the application of ionizing radiation

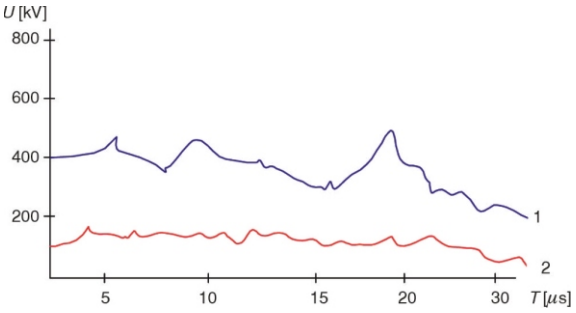

Figure 15. Stochasticity of the response of the gas surge arrester for high-voltage level; 1 – without the application of the source of ionizing radiation and 2 – with the application of ionizing radiation

Figure 15 shows the stochasticity of the response of the gas surge arrester for high voltage level without the application of the source of ionizing radiation and with the application of ionizing radiation. The effect of ionizing radiation almost completely cancels the stochastic peaks. This makes the gas surge arrester very reliable for insulation coordination at the high voltage level.

CONCLUSION

The paper examines the possibility of stabilizing the operation of gas surge arresters for insulation co-ordination at low, medium, and high voltage levels. This work is theoretical and experimental. In the theoretical part, the algorithm for determining the impulse characteristics and for the calculation of the DC breakdown voltage is derived. When calculating the breakdown voltage, the Townsend and streamer breakdown voltages were taken into account. Experiments conducted under well-controlled conditions showed that the source of ionizing radiation ^{241}Am (source of $\alpha + \beta$ radiation) completely stabilizes the gas surge arrester at the low voltage level, and somewhat less stabilizes the gas surge arrester at the medium voltage level. The source of ionizing radiation ^{241}Am least stabilizes the surge arrester at the high voltage level. For that reason, and for possible contamination of the environment with low voltage detectors with built-in radioactive sources, the use of these should

be avoided. For gas arresters, which perform insulation coordination at the medium and high voltage level, there is no danger of environmental contamination and their production with an additional source of ionizing radiation can be recommended.

AUTHORS' CONTRIBUTIONS

A. Jusić gave/proposed the idea for the experiment which was carried out by A. Jusić and Dj. Lazarević. All the authors analyzed the results and participated in preparation of the final version of the manuscript under supervision and guidelines of Dj. Lazarević and I. Turković.

REFERENCES

[1] Standler, R. B., *Protection of Electronic Circuits from Overvoltages*, Dover Books on Electrical Engineering, Mineola, New York, USA, 2002
[2] Beyer, M., *et al*., *Hochspannungtechnik, Theoretische und Praktische Grundlagen,* Springer-Verlag, Berlin, 1986
[3] Osmokrović, P., *et al*., Investigation of the Optimal Method for Improvement of the Protective Characteristics of Gas-Filled Surge Arresters – With/Without the Built-In Radioactive Sources, *IEEE Transactions on Plasma Science, 30* (2002), 5 I, pp. 1876-1880
[4] Howard, C., New Avalanche Diode for Transient Protection, Electronic Product Design, Bloomingdale, N. J., USA, 1983
[5] Vujišić, M., *et al*., Influence of Working Conditions on Over-Voltage Diode Operation, *Journal of Optoelectronics and Advanced Materials, 9* (2007), 12, pp. 3881-3884
[6] Saranya, A., *et al*., Role of Hexamine in ZnO Morphologies at Different Growth Temperature with Potential Application in Dye Sensitized Solar Cell, *Materials Science in Semiconductor Processing, 92* (2019), March, pp. 108-115
[7] Metwally, I. A., *et al.*, Lightning Transients in Low-Voltage Installations Inside Different Types of Class II Lightning Protection Systems, *IEEE Transactions on Power Delivery, 24* (2009), 2, pp. 930-938
[8] Metwally, I. A., Computation of Transient Overvoltages in Low-Voltage Installations During Direct Strikes to Different Lightning Protection Systems, *IEEE Transactions on Electromagnetic Compatibility, 49* (2007), 3, pp. 602-613
[9] Osmokrović, P., *et al*., Mechanism of Electrical Breakdown of Gases for Pressures from 10 -9 to 1 bar and Inter-Electrode Gaps from 0.1 to 0.5 mm, *Plasma Sources Science and Technology, 16* (2007), 13, art. no. 025, pp. 643-655
[10] Osmokrović, P., *et al*., Determination of Pulse Tolerable Voltage in Gas-Insulated Systems, *Japanese Journal of Applied Physics, 47* (2008), 12, pp. 8928-8934
[11] Pejović, M. M., *et al*., Kinetics of Positive Ions and Electrically Neutral Active Particles in Afterglow in Neon at Low Pressure, *Physics of Plasmas, 21* (2014), 4, art. no. 042111
[12] Rajović, Z., *et al*., Influence of SF6-N2 Gas Mixture Parameters on the Effective Breakdown Temperature of the Free Electron Gas, *IEEE Transactions on Plasma Science, 41* (2013), 12, art. no. 6645459, pp. 3659-3665
[13] Pejović, M., *et al.*, Processes in Insulating Gas Induced by Electrical Breakdown Responsible for Commercial Gas-Filled Surge Arresters Delay Response, *Vacuum, 137* (2017), March, pp. 85-91
[14] Vulević, B., *et al*., Evaluation of Uncertainty in the Measurement of Environmental Electromagnetic Fields, *Radiation Protection Dosimetry, 141* (2010), 2, art. no. ncq158, pp. 173-177
[15] Kartalovic, N. M., *et al*., Influence of the Synergy of Neutron and Gamma Radiation and Functional Aging on the Efficiency of a Hybrid Protection Circuit, *Nucl Technol Radiat, 37* (2022), 3, pp. 201-206
[16] Obrenović, M. D., *et al*., Statistical Review of the Insulation Capacity of the Geiger-Mueller Counter, *Nucl Technol Radiat, 33* (2018), 4, pp. 369-374
[17] Pejović, M. M., *et al*., Investigation of Post-Discharge Processes in Nitrogen at Low Pressure, *Physics of Plasmas, 19* (2012), 12, art. no. 123512
[18] Osmokrović, P., *et al*., The Validity of the General Similarity Law for Electrical Breakdown of Gases, *Plasma Sources Science and Technology, 15* (2006), 4, art. no. 015, pp. 703-713
[19] Dekić, S., *et al.*, Conditions for the Applicability of the Geometrical Similarity Law to Impulse Breakdown in Gases, I*EEE Transactions on Dielectrics and Electrical Insulation, 17* (2010), 4, art. no. 5539689, pp. 1185-1195
[20] Osmokrović, P., *et al*., The New Method of Determining Characteristics of Elements for Overvoltage Protection of low-Voltage System, *IEEE Transactions on Instrumentation and Measurement, 55* (2006), 1, pp. 257-265
[21] Pejović, M. M., *et al*., Investigation of Breakdown Voltage and Electrical Breakdown Time Delay in Air-Filled Tube in Presence of Combined Gas and Vacuum Breakdown Mechanism, *Vacuum, 86* (2012), 12, pp. 1860-1866
[22] Čaršimamović, A. S., *et al*., Low Frequency Electric Field Radiation Level Around High-Voltage Transmission Lines and Impact of Increased Voltage Values on the Corona Onset Voltage Gradient, *Nucl Technol Radiat, 33* (2018), 2, pp. 201-207
[23] Jusić, A., *et al*., Synergy of Radioactive ^{241}Am and the Effect of Hollow Cathode in Optimizing Gas-Insulated Surge Arresters Characteristics, *Nucl Technol Radiat, 33* (2018), 3, pp. 260-267
[24] Stanković, K., *et al*., Free-Electron Gas Spectrum Uniqueness in the Mixture of Noble Gases, *Contributions to Plasma Physics, 56* (2016), 2, pp. 126-133
[25] Osmokrović, P., *et al*., Stability of the Gas Filled Surge Arresters Characteristics Under Service Conditions, *IEEE Transactions on Power Delivery, 11* (1996), 1, pp. 260-266
[26] Osmokrović, P., *et al*., Influence of the Electrode Parameters on Pulse Shape Characteristic of Gas-Filled Surge Arresters at Small Pressure and Inter-Electrode Gap Values, *IEEE Transactions on Plasma Science, 33* (2005), 5 II, pp. 1729-1735
[27] Doličanin, E. Ć., *et al*., Monte Carlo Optimization of Redundancy of Nanotechnology Computer Memories in the Conditions of Background Radiation, *Nucl Technol Radiat, 33* (2018), 2, pp. 208-216
[28] Obrenović, M. D., *et al*., The Effects Induced by the Gamma-Ray Responsible for the Threshold Voltage Shift of Commercial p-Channel Power VDMOSFET, *Nucl Technol Radiat, 33* (2018), 1, pp. 81-86
[29] Perazić, L. S., *et al*., Application of an Electronegative Gas as a Third Component of the Working Gas in the Geiger-Mueller Counter, *Nucl Technol Radiat, 33* (2018), 3, pp. 268-274

[30] Osmokrović, P., *et al.*, Reliability of Three-Electrode Spark Gaps, Plasma Devices and Operations, 16 (2008), 4, pp. 235-245
[31] Belić, Č. I., *et al*., The Influence of the Magnetic Field on DC and the Impulse Breakdown of Noble Gases, *Materials, 12* (2019), 5, art. no. 752, 2019
[32] Pejović, M. M., *et al*., Experimental Investigation of Breakdown Voltage and Electrical Breakdown Time Delay of Commercial Gas Discharge Tubes, *Japanese Journal of Applied Physics, 50* (2011), 8, art. no. 086001
[33] Metwally, I. A., *et al*., Reduction of Lightning-Induced Magnetic Fields and Voltages Inside Struck Double-Layer Grid-Like Shields, *IEEE Transactions on Electromagnetic Compatibility, 50* (2008), 4, pp. 905-912
[34] Arandjelović, N. M., *et al.*, The Efficiency of Gas-Filled Surge Arresters in the Environment Contaminated by Non-Ionizing Radiation of Fusion Reactors, *Nucl Technol Radiat, 37* (2008), 1, pp. 51-56

Received on May 31, 2023
Accepted on June 27, 2023

Алија Р. ЈУСИЋ, Ђорде Р. ЛАЗАРЕВИЋ, Ирфан М. ТУРКОВИЋ

УТИЦАЈ ЈОНИЗУЈУЋЕГ ЗРАЧЕЊА НА СТОХАСТИЧНОСТ ПРЕНАПОНСКЕ ЗАШТИТЕ НА НИСКОМ, СРЕДЊЕМ И ВИСОКОМ НАПОНУ У ГАСНИМ ОДВОДНИЦИМА

У раду се разматра могућност побољшања техничких карактеристика гасних одводника пренапона за координацију изолације на нисконапонском, средњонапонском и високонапонском нивоу. Идеја за побољшање карактеристика гасног одводника пренапона заснива се на примени радиоактивног извора ^{241}Am у области катоде одводника пренапона. Интезивна јонизација алфа честицама повећава знатно број слободних електрона у међуелектродном простору чиме се скраћује време њиховог преласка у иницијалне електроне. Тиме се мења Пашенова крива гасног одводника пренапона, сужава и поравнава његова импулсна карактеристика и смањује стохастичност одзива гасног одводника пренапона. Све ово резултује знатним побољшањем карактеристика гасног одводника пренапона на свим напонским нивоима. Ово побољшање посебно је изражено у случајевима нисконапонских одводника пренапона. Рад је теоретско-експерименталног карактера. Експерименти су вршени под добро контролисаним лабораторијским условима. Комбинована мерна несигурност свих мерења била је прихватљива.

Кључне речи: гасни одводник пренапона, координација изолације, нисконапонски, средњонапонски и високонапонски нивои, побољшање одзива